CHEMISTRY
A EUROPEAN JOURNAL

Supporting Information

Structural changes and coordinatively unsaturated metal atoms on dehydration of honeycomb analogous microporous metal-organic frameworks

Pascal D. C. Dietzel*,[a] Rune E. Johnsen, Richard Blom, and Helmer Fjellvåg

[a] e-mail: pascal.dietzel@sintef.no

Contents

Table S1. Angles between the plane of the phenyl ring and the carboxylate group in CPO-27-Zn.

Scan	Temperature / K	∠(Phenyl–CO_2) / °	*d*(Zn1–O2) / Å
1	297	11.1(1)	2.014(2) & 2.346(2)
18	361	8.2(1)	2.061(2) & 2.310(2)
21	373	26.3(2)	2.076(2) & 2.489(3)
23	381	5.9(1)	2.092(2) & 2.176(2)
45	468	16.9(1)	2.111(2) & 2.128(2)

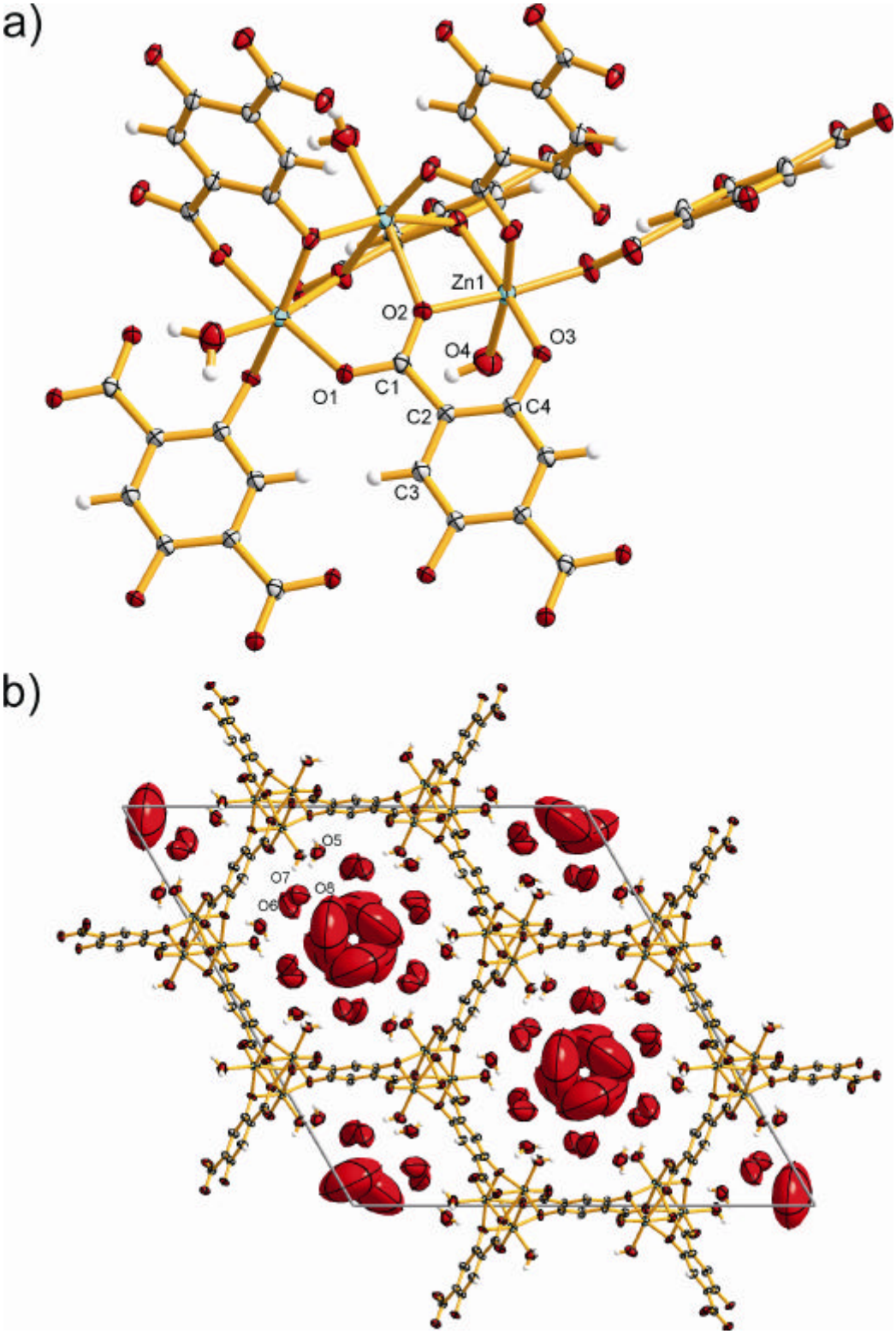

Figure S1. Single crystal X-ray structure of CPO-27-Zn at room temperature with atom labeling and thermal displacement ellipsoids (drawn at the 50% probability level): local surrounding of the zinc atom (a) and view along [001] (b).

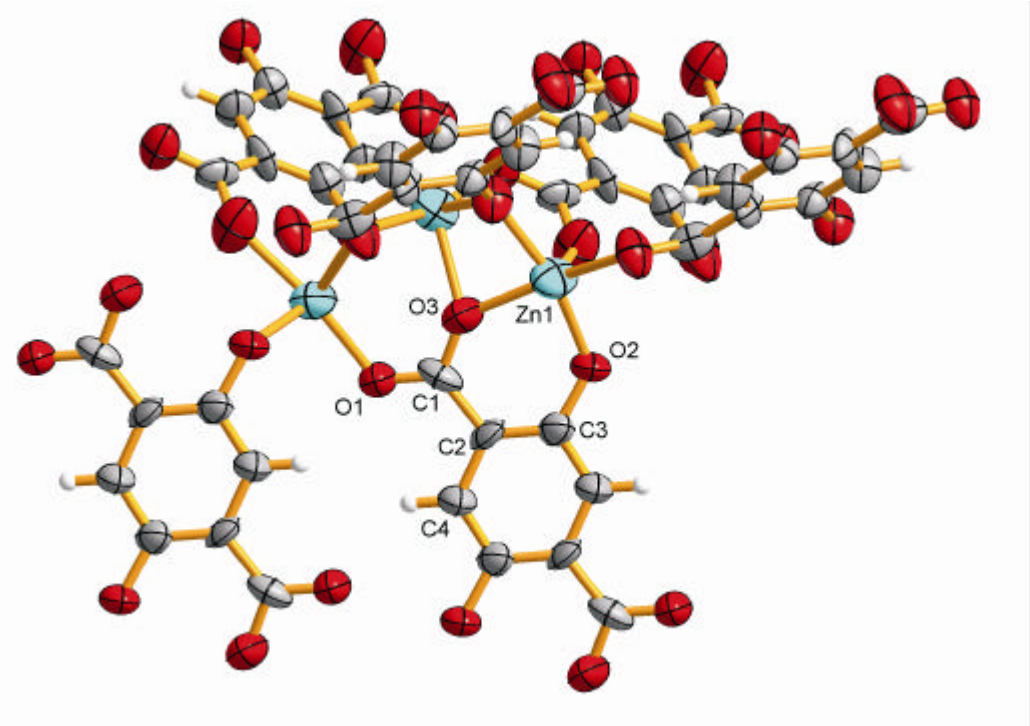

Figure S2. Single crystal X-ray molecular structure of CPO-27-Zn drawn along the backbone chain at 100°C with atom labeling and thermal displacement ellipsoids (drawn at the 50% probability level).

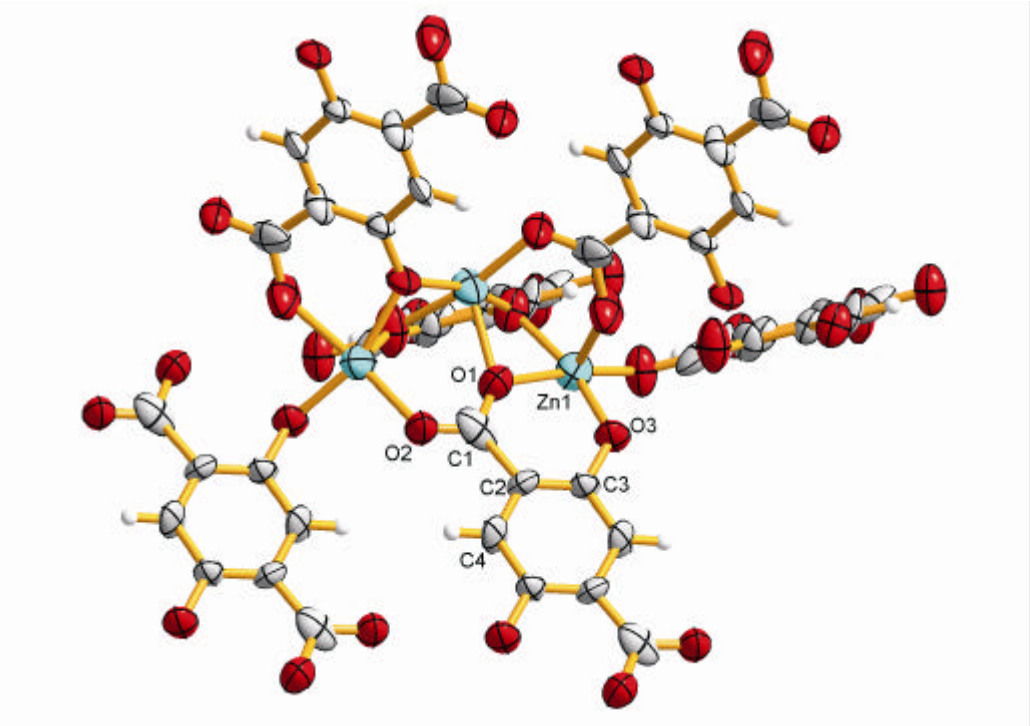

Figure S3. Single crystal X-ray molecular structure of CPO-27-Zn drawn along the backbone chain at 150°C with atom labeling and thermal displacement ellipsoids (drawn at the 50% probability level).

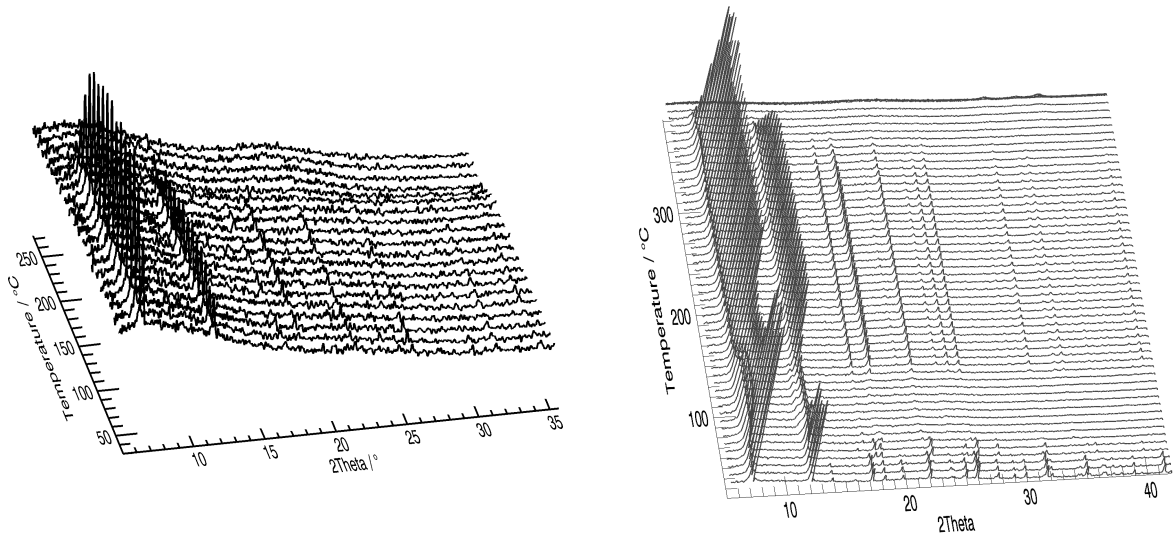

Figure S4. Variable temperature X-ray powder diffractograms of CPO-27-Co (left) and CPO-27-Zn (right) in nitrogen (lab data).

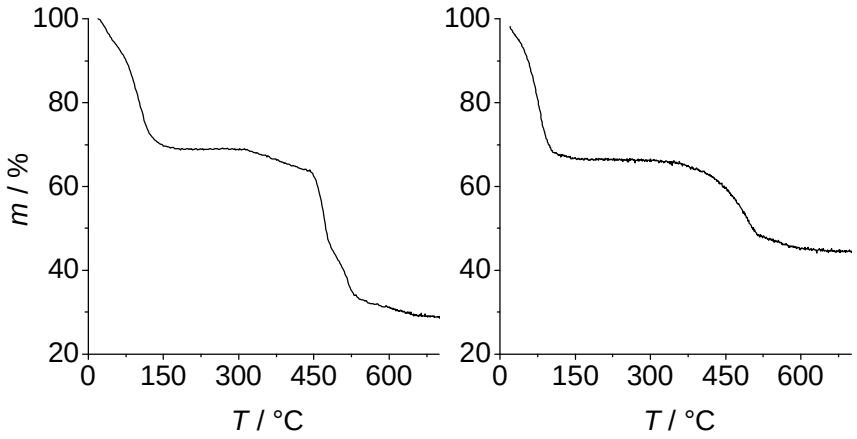

Figure S5. TG curve of CPO-27-Co (left) and CPO-27-Zn (right) in nitrogen showing the plateau of stability after solvent removal.

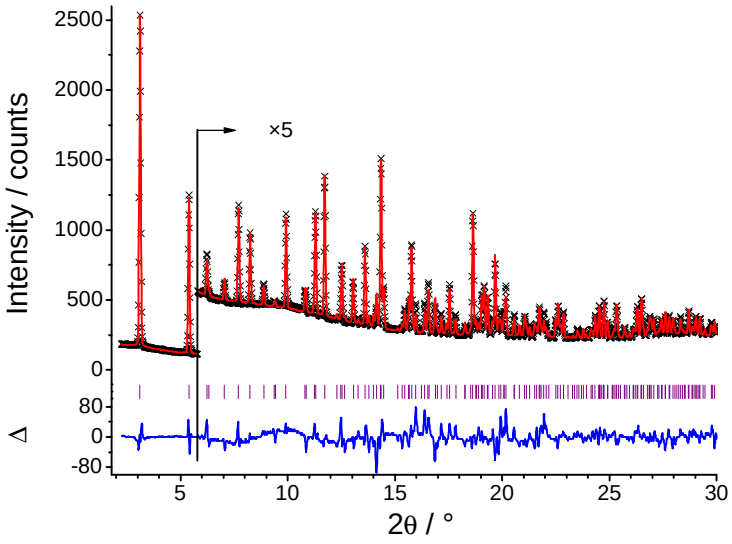

Figure S6. Scattered synchrotron radiation intensities of CPO-27-Co at 24°C as a function of the diffraction angle 2θ (crosses: observed pattern, red line: best Rietveld-fit profile, blue line: difference curve between observed and calculated profiles, magenta tick marks: reflection positions). Intensities and difference plot of the high angle part are enlarged by a factor of 5.

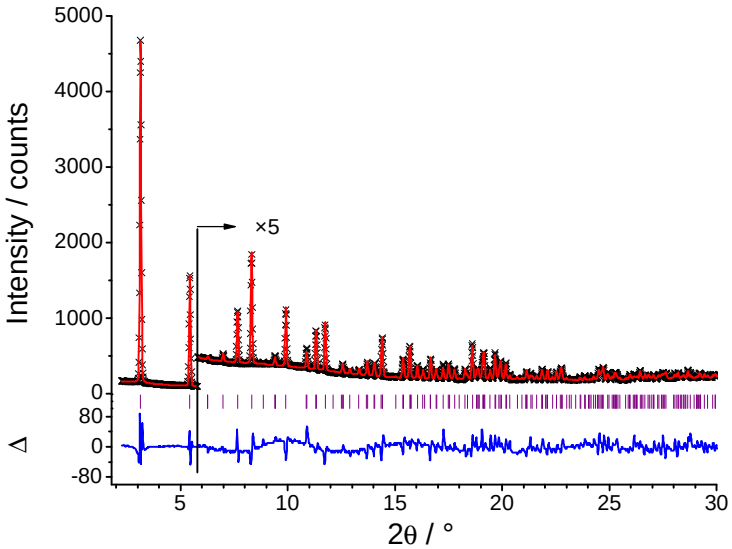

Figure S7. Scattered synchrotron radiation intensities of CPO-27-Co at 195°C as a function of the diffraction angle 2θ (crosses: observed pattern, red line: best Rietveld-fit profile, blue line: difference curve between observed and calculated profiles, magenta tick marks: reflection positions). Intensities and difference plot of the high angle part are enlarged by a factor of 5.

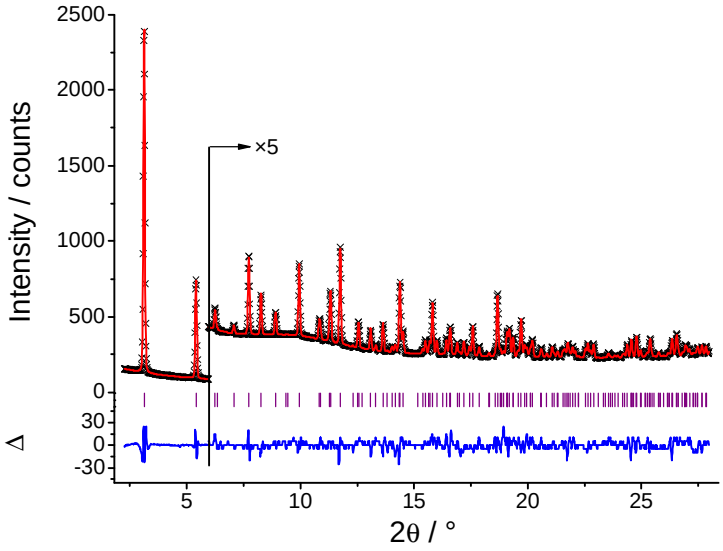

Figure S8. Scattered synchrotron radiation intensities of CPO-27-Zn at 24°C as a function of the diffraction angle 2θ (crosses: observed pattern, red line: best Rietveld-fit profile, blue line: difference curve between observed and calculated profiles, magenta tick marks: reflection positions). Intensities and difference plot of the high angle part are enlarged by a factor of 5.

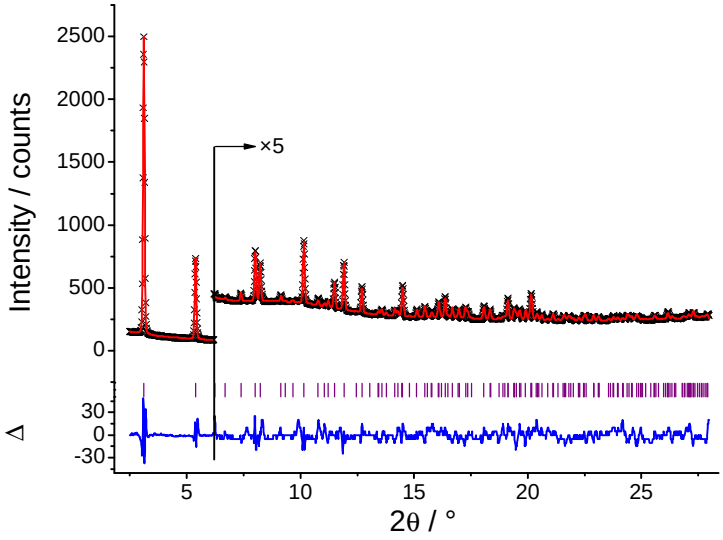

Figure S9. Scattered synchrotron radiation intensities of CPO-27-Zn at 100°C as a function of the diffraction angle 2θ (crosses: observed pattern, red line: best Rietveld-fit profile, blue line: difference curve between observed and calculated profiles, magenta tick marks: reflection positions). Intensities and difference plot of the high angle part are enlarged by a factor of 5.

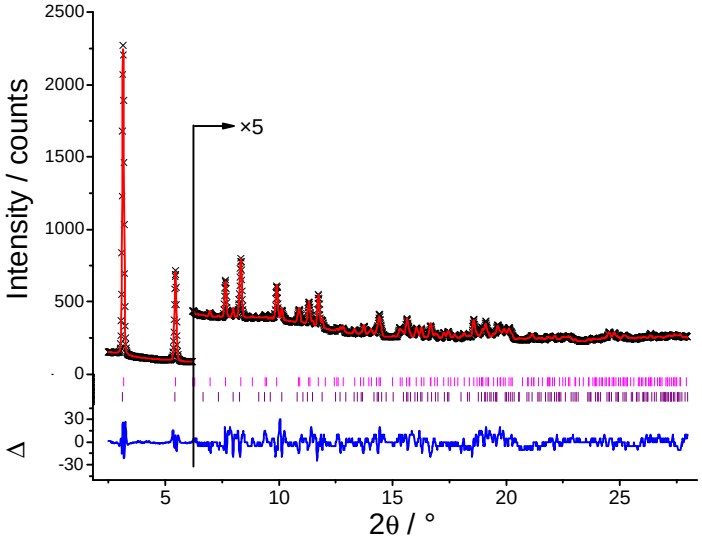

Figure S10. Scattered synchrotron radiation intensities of CPO-27-Zn at 108°C as a function of the diffraction angle 2θ (crosses: observed pattern, red line: best Rietveld-fit profile, blue line: difference curve between observed and calculated profiles, magenta tick marks: reflection positions). Intensities and difference plot of the high angle part are enlarged by a factor of 5.

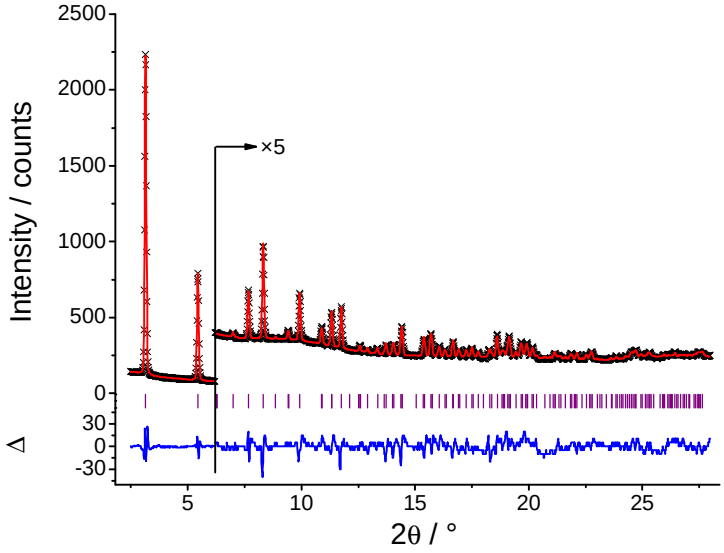

Figure S11. Scattered synchrotron radiation intensities of CPO-27-Zn at 195°C as a function of the diffraction angle 2θ (crosses: observed pattern, red line: best Rietveld-fit profile, blue line: difference curve between observed and calculated profiles, magenta tick marks: reflection positions). Intensities and difference plot of the high angle part are enlarged by a factor of 5.

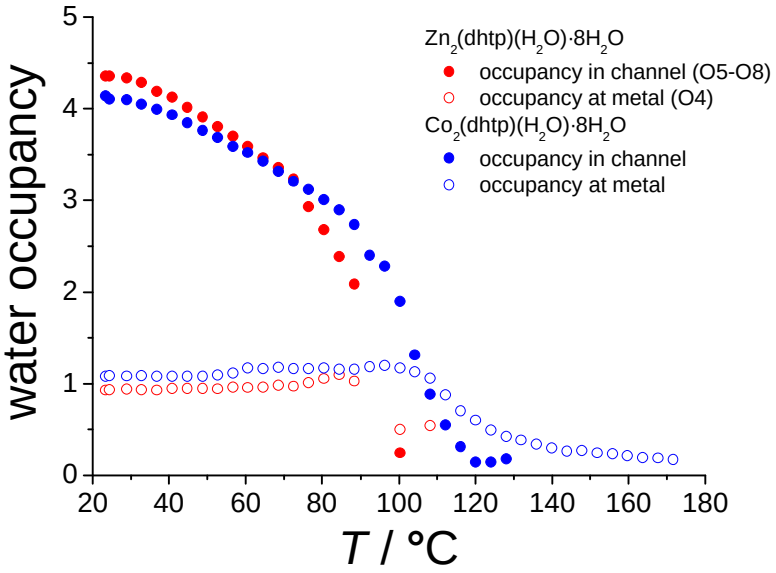

Figure S12. Occupation of bulk and metal coordinating water in CPO-27-Zn and CPO-27-Co.

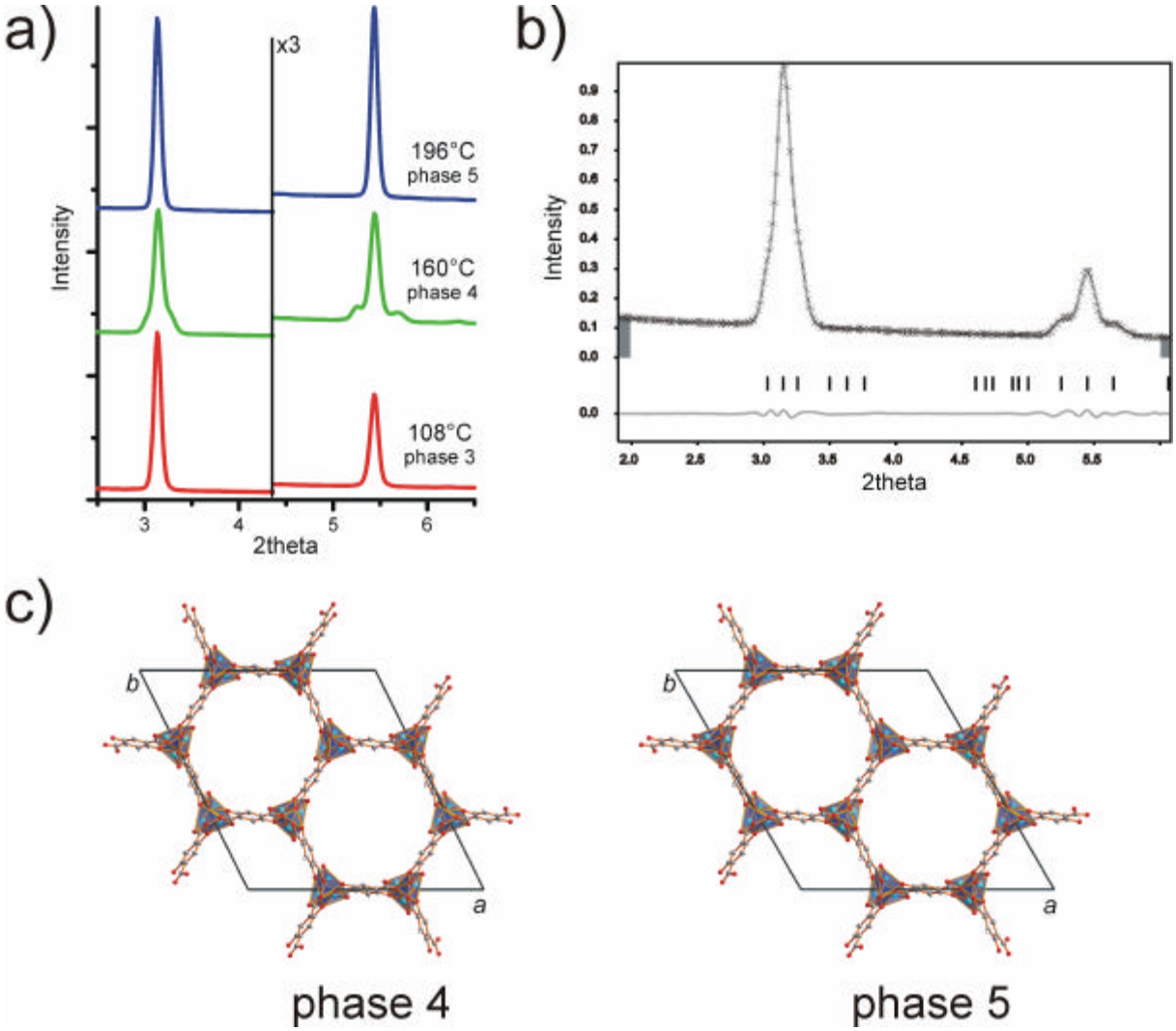

Figure S13. a) The first two reflections of CPO-27-Zn (300 and $2\bar{1}0$) split up on transition from phase 3 to phase 4. The splitting recedes upon transition to phase 5. b) Profile fit of the low angle range of a diffraction pattern of phase 4 in space group $P\bar{1}$ in which the initial reflections are split up into (110), ($1\bar{2}0$), and ($2\bar{1}0$) and (030), (300), and ($3\bar{3}0$), respectively. Thus, from this range values for *a*, *b*, and γ of 25.014 Å, 25.950 Å, and 116.34°, respectively, can be obtained. The profile fit was performed using JANA2000.[1] c) View of the crystal structure of phase 4 using the unit cell parameters obtained from the profile fit (employing fractional atom coordinates of phase 5, shown on the right for comparison).

References

(1) Petricek, V.; Dusek, M. *Jana2000. Structure Determination Software Programs*; Institute of Physics, Praha, Czech Republic, 2000.